Chapter 12
Adsorption Microcalorimetry as a Tool to Study the CO–Pt Interaction for PEMFC Applications: A Case Study

Georgeta Postole and Aline Auroux

Abstract To date, microcalorimetry of CO adsorption onto supported metal catalysts was mainly used to study the effects induced by the nature and the particle size of supported metallic clusters, the conditions of pretreatment and the support materials on the surface properties of the supported metallic particles. The present chapter focuses on the employ of adsorption microcalorimetry for studying the interaction of carbon monoxide with platinum-based catalyst aimed to be used in proton exchange membrane fuel cells (PEMFCs) applications.

12.1 Evolution and Types of Fuel Cell

Fuel cells are one of the oldest electrical energy conversion technologies known to man for more than 160 years. A fuel cell is a galvanic cell, in which the free energy of a chemical reaction is converted into electrical energy. Their development lacked a drive at the beginning, as primary energy sources were abundant, unrestricted, and inexpensive. After the second world war, this technology became the subject of intense research; one of the major factors that have influenced their development have been the increasing concern about the environmental consequences of fossil fuel use in production of electricity, and for the propulsion of vehicles. The historical development of fuel cells has been described by Carrete et al. [1], Litster et al. [2] and Boudghene Stambouli and Traversa [3]. In spite of the attractive system efficiencies and environmental benefits associated with fuel-cell technology, it is still a difficult task to transform the early scientific experiments into commercially viable industrial products. These problems have been often associated with the lack of appropriate

G. Postole (✉) · A. Auroux
Université Lyon 1, CNRS, UMR 5256, IRCELYON, Institut de recherches sur la catalyse et l'environnement de Lyon, F-69626 Villeurbanne Cedex, France
e-mail: georgeta.postole@ircelyon.univ-lyon1.fr

A. Auroux (ed.), *Calorimetry and Thermal Methods in Catalysis*,
Springer Series in Materials Science 154, DOI: 10.1007/978-3-642-11954-5_12,

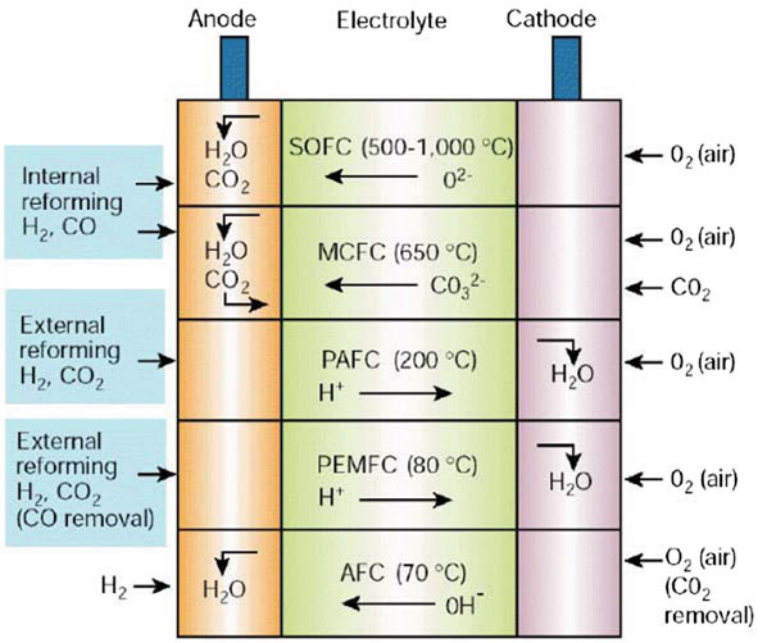

Fig. 12.1 Summary of fuel-cell types [5]

materials or manufacturing routes that would enable the cost of electricity per kWh to compete with the existing technology [4].

However, fuel cells may help to reduce our dependence on fossil fuels and diminish poisonous emissions into the atmosphere and that is the reason for their continuous development. For example, fuel cells using pure hydrogen as fuel produce only water, thus eliminating locally all noxious byproducts otherwise caused by electricity production.

Different types of fuel cells under active development are usually classified by the electrolyte employed as the ionic conductor in the cell, or by their operating temperature. Figure 12.1 summarizes the types of fuel cells in order of increasing operating temperature [5], while an overview of their characteristics is given in Table 12.1 [1, 3].

As it can be seen, low-temperature and high-temperature fuel cells can be distinguished. Low-temperature fuel cells are the Alkaline Fuel Cell (AFC), the Polymer Electrolyte Fuel Cell (PEMFC), and the Phosphoric Acid Fuel Cell (PAFC). The high-temperature fuel cells operate in the temperatures region from 500 to 1000 °C; two different types have been developed: the Molten Carbonate Fuel Cell (MCFC) and the Solid Oxide Fuel Cell (SOFC). They have the ability of using methane as fuel and thus present high inherent generation efficiency (45–60 % for common fuels such as natural gas, 90 % with heat recovery [3]).

Table 12.1 The characteristics of different fuel cells that have been realized and are currently in use and development

Fuel cells	AFC (Alkaline)	PEMFC (Polymer electrolyte membrane)	DMFC (Direct methanol)	PAFC (Phosphoric acid)	MCFC (Molten carbonate)	SOFC (Solid oxide)
Operating temperature ($^{\circ}C$)	<100	60–120	60–120	160–200	600–800	800–1000 low temperature (500–600) possible
Anode reaction	$H_2 + 2OH^- \rightarrow 2H_2O + 2e^-$	$H_2 \rightarrow 2H^+ + 2e^-$	$CH_3OH + H_2O \rightarrow CO_2 + 6H^+ + 6e^-$	$H_2 \rightarrow 2H^+ + 2e^-$	$H_2 + CO_3^{2-} \rightarrow H_2O + CO_2 + 2e^-$	$H_2 + O^{2-} \rightarrow H_2O + 2e^-$
Cathode reaction	$1/2O_2 + H_2O + 2e^- \rightarrow 2OH^-$	$1/2O_2 + 2H^+ + 2e^- \rightarrow H_2O$	$3/2O_2 + 6H^+ + 6e^- \rightarrow 3H_2O$	$1/2O_2 + 2H^+ + 2e^- \rightarrow H_2O$	$1/2O_2 + CO_2 + 2e^- \rightarrow CO_3^{2-}$	$1/2O_2 + 2e^- \rightarrow O^{2-}$
Electrolyte	Potassium hydroxide (KOH)	Polymer, proton exchange membrane	Polymer	Phosphoric acid	Molten salt such as nitrate, sulphate, carbonates…	Ceramic as stabilized zirconia and doped perovskite
Charge carrier in the electrolyte	OH^-	H^+	H^+	H^+	CO_3^{2-}	O^{2-}

(continued)

Table 12.1 (continued)

Fuel cells	AFC (Alkaline)	PEMFC (Polymer electrolyte membrane)	DMFC (Direct methanol)	PAFC (Phosphoric acid)	MCFC (Molten carbonate)	SOFC (Solid oxide)
Fuel	Hydrogen or hydrazine	Hydrogen	Liquid methanol	Hydrogen	Hydrogen, carbon monoxide, natural gas, propane	Hydrogen, hydrocarbons, natural gas, renewable fuels
Applications	Transportation, space, military, energy storage system			Combined heat and power for decentralized stationary power systems	Combined heat and power for decentralized stationary power systems and for transportation (train, boats, …)	
Realized power	Small plants 5–150 kW modular	Small plants 5–250 kW modular	Small plants 5 kW	Small-medium plants 50 kW–11 MW modular	Small power plants 100 kW–2 MW modular	Small power plants 100–200 kW
Efficiency (%)	50–55	40–50	40–55	40–50	50–60	45–60

Not mentioned in this classification is the Direct Methanol Fuel Cell (DMFC) working at 60–120 °C and using methanol as a fuel. There are also other types of fuel cells (e.g. air-depolarised cells, sodium amalgam cells, alkali metal-halogen cells, etc.) which are less employed, but that can possibly find a specific application in the future.

The basic structure of all fuel cells is similar: the cell consists of two electrodes which are separated by the electrolyte and which are connected in an external circuit. The electrodes are exposed to gas or liquid flows to supply the electrodes with fuel or oxidant (e.g. hydrogen or oxygen). As it can be seen in Table 12.1, the anode reaction in fuel cells is either the direct oxidation of hydrogen (low temperature fuel cells) or the oxidation of methanol (DMFC). An indirect oxidation via a reforming step can also occur in the case of high temperature operation fuel cells. The cathode reaction is oxygen reduction, in most cases from air.

Both the low-temperature and the high-temperature fuel cells have their advantages and disadvantages depending on the application. For example, among the fuel cells used for transportation, the high-temperature fuel cells (such as solid oxide or molten carbonate cells) present advantages for the use in ships or locomotives in which frequent on/off cycling is not required. They allow more flexibility in fuel selection and may be used without a reformer. The high-grade waste heat is more easily used in a thermally integrated system. Conversely, the low-temperature fuel cells, such as polymer electrolyte or alkaline, may be a better choice for passenger cars to which rapid start-up and wide power range are important [6].

By far the greatest research interest throughout the world has focussed on proton exchange membrane (PEM) and solid oxide (SO) cell stacks. PEMFCs are well advanced type of fuel cells that has found widespread area of use, especially in transportation applications, distributed generation (DG) units and portable electronic equipments [7]. Some of the key advantages of PEMFC systems over the other competitive types of fuel cells for its potential market competitiveness arise from [8]:

- PEMFCs can operate at relatively low temperatures.
- PEMFCs are tolerant to CO_2; so they can use the atmospheric air.
- PEMFCs have high voltage, current and power density.
- PEMFCs can work at low pressure (1 or 2 bars), which enhances security.
- PEMFCs have a good tolerance to the difference of pressure of the reactants.
- PEMFCs are compact and robust and have a simple mechanical design.
- PEMFCs use stable building materials.

12.2 Proton Exchange Membrane Fuel Cells

PEM fuel cells use a proton exchange membrane as an electrolyte and operates at low-temperatures, between 60 and 120 °C. From various types of fuel cells, PEMFCs are suitable choice for both stationary and portable applications due to their fast start up,

high power density, suitability for discontinuous operation as well as low operating temperature [8–10]. Their components and related functions are well described in a recent review [9]. The first application of a PEM fuel cell was in the 1960s as an auxiliary power source in the Gemini space flights. It was also used to provide the astronauts with clean drinking water. The membrane used was a polystyrene sulfonate (PSS) polymer, which has been proven do not be enough stable. Advances in the PEMFCs technology were stagnating until the late 1980s when the fundamental design underwent significant reconfiguration. A major breakthrough in this field came with the use of Nafion® or Dow® membranes, possessing a higher acidity and conductivity and being more stable than the polystyrene sulfonate membranes [1, 2].

Figure 12.2 presents the principle of a single proton exchange membrane fuel cell fed with hydrogen which is oxidized at the anode, and oxygen that is reduced at the cathode [1]. The protons released during the oxidation of hydrogen are conducted through the proton exchange membrane (the electrolyte) to the cathode. Since the membrane is not electrically conductive, the electrons released from the hydrogen travel along the electrical detour provided and an electrical current is generated. The reaction product is water, which is formed at the cathode [2].

In order to be efficient enough, the electrochemical reactions that take place in fuel cell must be catalyzed. To date, platinum has proven to be the best catalyst for both the hydrogen oxidation (anode) and the oxygen reduction (cathode) reactions. For PEM fuel cell applications, platinum is usually implemented in the form of Pt/C catalysts because of its significantly higher surface area compared with that of platinum black catalysts resulting in its cost reduction [5, 11].

The oxidation of hydrogen occurs readily on Pt-based catalysts involving the adsorption of the gas onto the catalyst surface followed by a dissociation of the molecule and electrochemical reaction to two hydrogen ions as follows:

$$2Pt_{(s)} + H_2 \rightarrow Pt{-}H_{ads} + Pt{-}H_{ads} \tag{12.1}$$

$$Pt{-}H_{ads} \rightarrow H^+ + e^- + Pt_{(s)} \tag{12.2}$$

where $Pt_{(s)}$ is a free surface site and Pt–H_{ads} is an adsorbed H-atom on the Pt active site.

The overall reaction of hydrogen oxidation is:

$$H_2 \rightarrow 2H^+ + 2e^- \tag{12.3}$$

The rate of the hydrogen oxidation process at the Pt-based catalyst at 80 °C is very high, as long as the catalyst surface is not contaminated by adsorbed impurities.

The highest performing PEMFC systems employ pure hydrogen as the fuel, but for many applications, especially mobile, pure hydrogen is not yet a viable option due to the technical difficulty of on-board storage and refuelling. Currently, the most viable technology for on-site H_2 generation is reforming technology (e.g. steam reforming, partial oxidation or autothermal reforming) of hydrocarbons such as methanol,

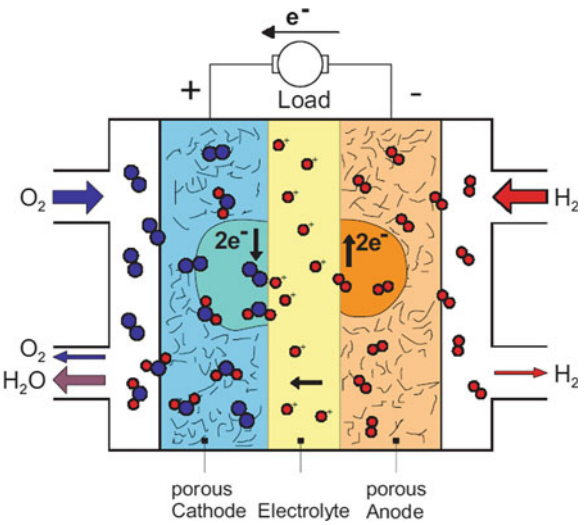

Fig. 12.2 Schematic presentation of a single typical proton exchange membrane fuel cell [1]. On the anode, hydrogen gas is catalytically disassociated according to the reaction $H_2 \rightarrow 2e^- + 2H^+$. The hydrogen ions pass through the polymer electrolyte to the cathode where oxygen, in most cases from air, is reduced ($O_2 + 4e^- \rightarrow O^{2-}$). The overall reaction is: $H_2 + 1/2O_2 \rightarrow H_2O$

gasoline or natural gas and alcohols that are readily available through existing distribution channels [12]. Accordingly, the use of hydrocarbon or alcohol fuels requires an external fuel processor (reformer) to be incorporated into the system. This item not only increases the complexity and cost of the fuel cell system, but also decreases the overall efficiency. The use of reformate fuel presents special challenges for a PEM fuel cell in terms of system efficiency, reliability, and durability. Many of these issues can be attributed to the detrimental effects of impurities such as CO, CO_2, NH_3 and H_2S obtained as the by-products of the reforming process [13]. The hydrogen impurities due to manufacturing process are brought along with the fuel feed stream into the anode of a PEMFC stack, causing performance degradation, and sometimes permanent damage of the membrane electrode assemblies [14–16]. The effect of different contaminants including: fuel impurities (CO,CO_2, H_2S, and NH_3), air pollutants (NO_x, SO_x, CO, and CO_2), and cations resulting from the corrosion of fuel cell stack system components (such are Fe^{3+} and Cu^{2+}) on the efficiency of PEM fuel cells was recently reviewed by Cheng et al. [17]. It was found that even trace amounts of impurities present in either fuel or air streams or fuel cell system components could severely poison the anode, membrane, and cathode, particularly at low-temperature operation, what results in dramatic performance drop. Thus, elucidation of the degradation mechanism of anode or cathode reactions by impurity materials in polymer electrolyte fuel cells (PEMFCs) is a crucial topic, to attain its longevity.

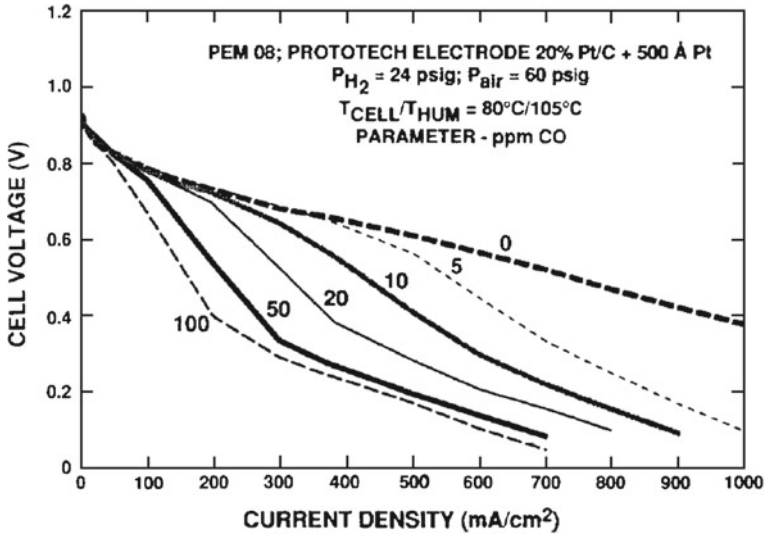

Fig. 12.3 The performance losses caused by trace amounts (from 5 to 100 ppm) of carbon monoxide in the fuel stream [6]

Poisoning of the anode catalyst is caused primarily by carbon monoxide, either brought into the cell with the fuel feed stream or generated in situ by the reduction of CO_2 [9, 17–19]. The hydrogen produced by steam reforming, contains more than 1 % of CO [6, 13, 20]. Since a PEMFC cannot tolerate such high CO levels, the carbon monoxide content is reduced through a series of high- and low-temperature water-gas-shift (WGS) and preferential oxidation (PROX) reactions to bring the CO level to less than 10 ppm [21]. However, due to the typical low temperature of operation (ca. 80 °C) and the choice of Pt as the electrocatalyst, the CO-poisoning effect could significantly affect the long-term performance of the PEMFC stack, even at this low CO level as it can be seen in Fig. 12.3 [6, 22, 23]. CO poisoning on Pt electrocatalysts becomes more severe with increases in CO concentration and exposure time. For example, Fig. 12.3 illustrates typical fuel cell stack polarization curves obtained at 80 °C in both the absence and presence of various concentrations of CO [6]. The figure indicates that the CO impurities from fuel streams, even at a level of a few ppm, can cause a substantial degradation in cell performance, especially at high current densities.

This problem is therefore particularly severe with fuel feed streams derived from the steam reforming of hydrocarbons, methanol or other liquid fuels, and is of lesser concern when the PEMFC operates on neat hydrogen. Nevertheless, the level of CO which brings about significant poisoning at the hydrogen anode in a PEMFC is so small (several parts per million) that even in the case of relatively pure hydrogen feeds, e.g., bottled hydrogen of nominal 99.99 % purity, some long-term platinum anode performance loss has been observed [9]. Overcoming the CO poisoning problem is

thus of paramount interest and needs to be addressed in order to make reformate gas a viable fuel for PEM fuel cells. Extensive research has focused on gaining a better understanding of poisoning effect that CO has on PEMFC performance. Baschuk and Li [24] reviewed the CO poisoning of platinum electrocatalyts used in PEM fuel cells in terms of characteristics, mechanism, mitigation, and theoretical models. Many electrochemical, spectroscopic and theoretical studies [23, 25–31] have been employed to investigate the CO adsorption process on platinum and Pt-based electrocatalysts, including in situ attenuated total reflectance-Fourier transform infrared (ATR-FTIR) study [32, 33], CO isotope exchange experiments [34], cyclic and stripping voltammetry [35], etc. Although these studies provide valuable information for the design of new catalysts, extrapolations of the conclusions with respect to the CO tolerance to the real systems are not straightforward, mainly because of reaction conditions that are different from the actual PEM fuel cell operating environment. However, it has been shown without doubts that the CO poisoning effect was strongly related to the concentration of CO, the exposure time to CO, the cell operation temperature, and anode catalyst types.

12.3 CO Adsorption Microcalorimetry on Pt-Based Materials: Literature Survey

Gas-solid interactions are fundamental for the understanding of adsorption, which is the first step in a variety of processes in surface science. The characterization of many gas-solid surface processes and the study of the gas interaction with heterogeneous surfaces (surfaces composed of different kinds of sites) are therefore important aspects. One of the challenges in the field of gas-solid interactions is to envisage methods for the determination of the energetic topography of heterogeneous substrates from adsorption experiments. In this context, the adsorption microcalorimetry technique coupled to volumetry is a powerful tool able to supply information about the strength of gas-surface interactions [36–39]. Moreover, the adsorption microcalorimetry also provides a direct measurement of heat of adsorption and their evolutions with the coverage and can contribute in the study of all phenomena which can be involved in one catalyzed process, e.g. activation/deactivation of the catalyst, coke production, pore blocking, sintering, and adsorption of poisoning in the feed gases [40, 41].

Chemisorption of carbon monoxide on transition metal surfaces (either single crystals or supported clusters) is a tool of general use to study the active sites present over this type of solid surfaces [42]. CO adsorption on noble metals has been the subject of a large number of papers. For instance, the adsorption behaviour of CO on surfaces of Pt single crystals, polycrystalline Pt films, and supported Pt catalysts has been discussed in terms of adsorbed species or adsorption structures formed during interaction of CO with the metal surface.

The adsorption of CO on a series of platinum based catalysts was also carried out by microcalorimetry technique, supplying information about the number, the strength distribution and the heat associated to the carbon monoxide adsorption on available Pt surface sites. Table 12.2 lists some literature reports on the average heats of CO adsorption over different platinum supported catalysts. In this table, the experimental data on powdered catalysts were collected from the vicinity of room temperature up to 130 °C. Prior to CO adsorption, the samples were reduced at 200 or 500 °C under hydrogen flow.

In these literature reports [43–58], the data obtained by adsorption microcalorimetry are considered together with those obtained from complementary techniques (i.e. infrared spectroscopy, temperature programmed desorption, X-ray photoelectron spectroscopy) in order to elucidate the influence of loading and dispersion of Pt, type of support material and the reduction temperature, on energetics and mechanism of CO adsorption on supported Pt catalysts for a better understanding of their catalytic performances.

For example, by examining the initial and differential heats of adsorption measured on Pt/Al_2O_3 powders calcined at different temperatures, Uner and Uner [50] concluded that CO adsorption processes is not structure-sensitive. CO heats of adsorption values obtained by the authors are plotted against carbon monoxide coverage in Fig. 12.4. The heat of adsorption data for all catalysts fell on the same curve,

Table 12.2 Literature data of CO adsorption over supported Pt surfaces

Catalyst	Pt (wt%)	Temperature of adsorption (°C)	Average heat of adsorption (kJ/mol)	Reference
Pt/C (Norit RX-3)	0.22	27	115	43
Pt/C (Vulcan)	5.00	27	110	44
Pt/graphite	2.00	57	115	45
Pt/C	1.00	25	80	46
$PtSn/TiO_2$	2.00	25	105	47
Pt/TiO_2	2.00	27	90	48
Pt/A_2O_3	1.88	25	120	49
Pt/Al_2O_3	2.00	30	135	50
Pt/Al_2O_3 nano-fibre	2.91	30	120	51
Pt/η-Al_2O_3	2.10	47	100	48
Pt/Al_2O_3	3.00	57	130	42,52
Pt/Al_2O_3	5.00	50	130	53
Pt/SiO_2	10.00	27	135	54
Pt/SiO_2	2.10	47	113	48
Pt/SiO_2	1.20	130	130	55,56
$Pt/SiO_2–Al_2O_3$	1.50	27	115	48
Pt/NaX zeolite	1.00	27	130	57
Pt/K-L zeolite	1.00	130	120	58
Pt/K-ZSM5 zeolite	1.00	130	110	58

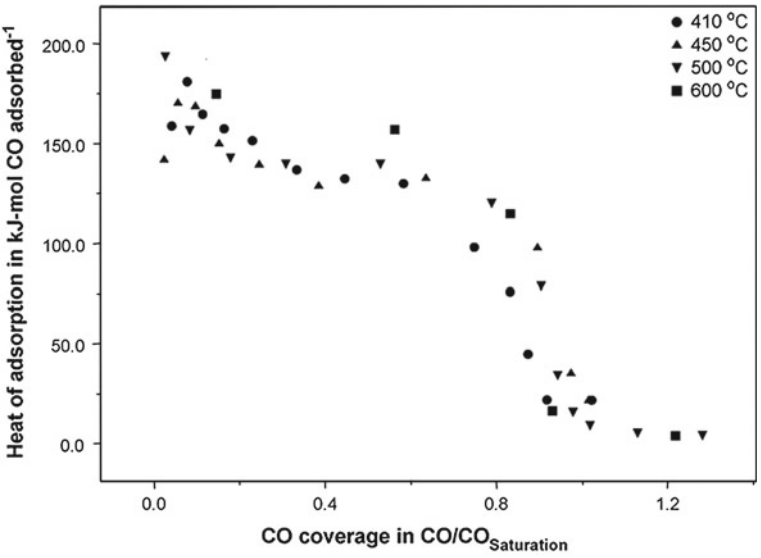

Fig. 12.4 Differential heat of carbon monoxide adsorption at 30 °C over 2 % Pt/γ-Al_2O_3 reduced under hydrogen at 270 °C. The temperatures indicate the calcination temperature of the catalysts [50]

but the adsorbed gas amounts decreased with increasing the calcinations temperature in agreement with the decrease in metal dispersions.

Serrano-Ruiz et al. [49] used the adsorption microcalorimetry of CO at room temperature, X-ray photoelectron spectroscopy (XPS), and ^{119}Sn Mössbauer spectroscopy to study the effect of adding Sn to Pt/CeO_2–Al_2O_3 and Pt/Al_2O_3 catalysts. Microcalorimetric analysis indicated that adding cerium caused the appearance of a more heterogeneous distribution of active sites, whereas adding tin led to a higher homogeneity of these sites. The influence of reduction conditions on the Pt–CO adsorption strength have also been investigated in detail for Pt/Al_2O_3. The authors [49] observed that the catalyst reduction at higher temperature caused a decrease of the initial CO adsorption heat (from 140 to 120 kJ/mol) and of CO saturation coverage from 55 to 45 $\mu mol_{CO}/g_{cat}$. Thus a higher homogeneity of the surface metal atoms for CO adsorption was reported when catalyst was reduced at 500 °C. The higher initial heat of adsorption obtained in the sample reduced at low temperature (200 °C) was attributed to the interaction of CO with highly unsaturated metal atoms at corners and edges. The decrease of the total amount of CO adsorbed with increasing the pretreatment temperature was explained to be due to sintering of the Pt particles after high-temperature reduction.

The CO adsorption microcalorimetry was also used to explain the promoting effect of Pt in bimetallic Ni–Pt catalysts supported on alumina nano-fibre (Alnf) tested for the liquid phase reforming of sorbitol to produce hydrogen [51]. The differential heat of adsorption for Ni–Pt/Alnf reduced to around 111 kJ/mol, which was 12 and

6 kJ/mol lower than Pt/Alnf and Ni/Alnf respectively. This is substantial because reducing the CO binding strength can avoid the poisoning of the active metal sites. These results suggest that in the case of bimetallic catalysts there was a reduction in the number of strong CO-adsorption sites.

The influence of support on CO–Pt interaction was studied by Vannice et al. [48] using adsorption microcalorimetry. The supports used were SiO_2, η-Al_2O_3, SiO_2–Al_2O_3, and TiO_2. The studied catalysts possessed a range of differential heats of CO adsorption at 27 °C between 88 and 135 kJ/mol (21 and 32 kcal/mol) with the Pt/TiO_2 sample having the lowest values. This variation in the values of differential heats of adsorption appears to be a strong function of crystallite size, with weaker Pt–CO bonding occurring as Pt dispersion increases.

Although one of the most commonly used catalysts today is Pt/Al_2O_3, the use of carbonaceous materials as catalyst supports is continuously increasing. Their porous texture can be easily tailored, yielding high surface-area supports where the active phase can be well dispersed, and with the required pore-size distribution to facilitate the diffusion of reactants and products to, and from, the active phase [59]. In the case of noble-metal-based catalysts, the metal dispersion in the final catalyst depends on a number of factors: porous texture of the support, nature of the metal precursor, types and amount of surface complexes on the support, etc. [60]. Guerrero-Ruiz et al. [45] applied CO adsorption microcalorimetry to study the factors affecting the Pt dispersions over high surface area graphite. Using different carbon supports (e.g. with, and without, oxygen surface groups) and different platinum precursors (H_2PtCl_6 and $Pt(NH_3)_4(OH)_2$) for the catalysts preparation, the authors showed that adsorption microcalorimetry is one useful tool to provide some evidence concerning the specific interaction that takes place between graphite carbon and metal particles. Thus, microcalorimetry of CO adsorption evidences that the presence of oxygen surface groups diminishes the metal-support interaction having as results lower differential heats of CO adsorption.

Heat of adsorption of a gas on a solid is, in general, composed of several contributions, including energy of the formed surface bond, energy associated with perturbation (or even dissociation) of the adsorbate, energy of interactions between the adparticles and energy associated with the surface relaxation or rearrangement [61]. Thus, in the basic research of adsorption, it is frequently desirable to separate the individual effects. In order to facilitate such a separation, and to minimize the complicating effects of the polycrystallinity and contamination of the surface, the adsorption microcalorimetry is often carried out for the surfaces of well defined crystal structure. Such surfaces can be obtained in the forms of metal filaments, vacuum-evaporated thin films, and single crystals of metals. The comparison of adsorption heats obtained by microcalorimetry over supported metallic clusters with those determined over metallic single crystals can help to understand the actual surface structure of the metal aggregates, and then their catalytic properties. Moreover, the adsorptive properties of CO on platinum single crystals can provide a better understanding of CO–Pt interaction, what can bring important information for designing of new catalysts and for the purpose of understanding the activity of Pt metal nanoparticles employed in fuel cells in the size range of few nanometers. Information concerning the CO

adsorption on single platinum crystals has been mainly gained from kinetic studies and from spectroscopic techniques, whereas the direct determination of adsorption heats has been less applied. Karmazyn and coworkers [62] studied, for example, the chemisorption of CO on the stepped Pt{2 1 1} surface using first-principles density functional theory (DFT) and microcalorimetry experiments. The heat of adsorption of CO on Pt{2 1 1} were measured at room temperature as a function of coverage and an initial heat of adsorption of 185 kJ/mol was found. Yeo et al. [63, 64] reported the values of 180 and 215 kJ/mol for the initial CO heats of adsorption on unsupported Pt{1 1 1} and Pt{1 0 0}, respectively. It can be observed that the heat of adsorption data obtained for Pt single crystal surfaces with two different orientations is different, beyond experimental errors.

The insight into the data presented in Table 12.2 gives evidence that it is difficult to elucidate the structure dependency of CO chemisorptions from the heats of adsorption found over supported catalysts. Even though, based on literature reports it can be concluded that the adsorption microcalorimetry, although not widely used, is a powerful technique for surface characterization of supported metal clusters, because it enables obtaining data concerning the strength of interaction and population of active sites. Concerning CO–Pt interaction, it is evident that CO is chemisorbed on all Pt-based catalysts (average heats of adsorption is higher than 100 kJ/mol, see Table 12.2). The differential heat profiles are usually characterised by a plateau of nearly constant heat of adsorption at low CO coverage, followed by an abrupt decrease as the surface saturation limit is reached.

12.4 The CO Poisoning Effects on Pt/C Studied by Adsorption Microcalorimetry: A Case Study

However, although the determination of the heat of adsorption of carbon monoxide on platinum have been reported in the literature (Table 12.2), the possible use of adsorption microcalorimetry as an available technique for giving valuable information in PEM fuel cells studies has not been reported. In what follows, recent results from our work in the field of microcalorimetry of CO adsorption on Pt/C catalysts are presented [65–67]. The catalysts used in these studies were different commercial carbon-supported platinum, with high Pt loading, aimed to be used in PEMFCs applications. Particular emphasis on the sample history (preparation method, the support material, the metal loading) and the pre-treatment of the catalysts on the CO poisoning effect on supported platinum is paid.

The results of CO adsorption microcalorimetry described in this overview were collected with a differential and isothermal microcalorimeter (Tian–Calvet Microcalorimeter) linked to a static volumetric system. The equipment permits the introduction of successive small doses of CO onto the catalyst. Both the calorimetric and the volumetric data were stored and analyzed by microcomputer processing. The obtained data are presented as differential heats versus the amount of CO adsorbed

while the amount of gas adsorbed at constant temperature are plotted as a function of the equilibrium pressure, thus giving adsorption isotherms. By using microcalorimetry, the structure sensitivity of hydrogen and carbon monoxide adsorption was investigated by using the Pt/C commercial catalysts with different Pt loading on carbon support. The studied catalysts were thus Pt/C powders provided by E-Tek (lot#E 1280702, 16.8 wt% Pt), Tanaka (lot 103-1341R, 24.5 wt% Pt), and Johnson Mathhey (lot 128372001, 16.6 wt% Pt) companies. As in a PEM fuel cell CO comes at the anode surface as an impurity in the hydrogen flow, H_2 adsorption microcalorimetry was also applied for a better understanding of CO effect on Pt based catalysts.

Due to higher CO poisoning effect at lower temperatures, it is important to know its effect at room temperature at which the start-up of the fuel cell system takes place. It is why the adsorption studies were carried out at two different temperatures: near room temperature (30 °C) and at 80 °C (the PEMFCs operation temperature). Prior to the adsorption experiments, the catalysts were reduced under static hydrogen (27 kPa) at 25, 100 or 200 °C.

The obtained microcalorimetric results showed that both H_2 and CO can be chemisorbed on all Pt/C catalysts. Indifferent of their provenience (different carbon support and different method of preparation), Pt/C exhibited significantly higher differential heats of carbon monoxide adsorption in comparison with hydrogen adsorption as can be seen in Fig. 12.5.

It is thus evident that in case of co-adsorption of these two gases (similar situation to that in fuel cell), CO will be primarily adsorbed. In addition, the adsorbed amount of CO is much higher than the amount of adsorbed H_2, which means that the Pt based catalysts present a larger number of sites active for carbon monoxide adsorption, in comparison with those active for hydrogen adsorption. By comparison with results

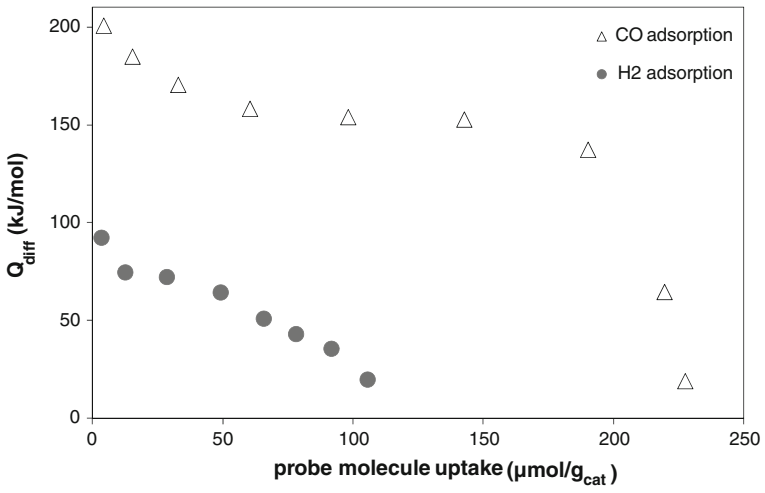

Fig. 12.5 Differential heats of H_2 and CO adsorption at 30 °C as a function of surface coverage for Pt/C sample (E-Tek, lot#E 1280702) pre-treated at 25 °C in static hydrogen (27 kPa)

obtained for different Pt/C catalysts [65, 67], no structure dependency was observed for hydrogen initial heats of adsorption. Similar values were obtained for hydrogen adsorption for all Pt/C catalysts, in good agreement with previously published values for supported and unsupported platinum catalysts [56, 58, 68–70]. Higher values of CO adsorption heats (average values ranged from 135 to 155 kJ/mol for the three tested catalysts) where observed when compared with those reported in Table 12.2.

The difference observed in the adsorption heats values could be attributed to different experimental conditions used, different loading of Pt and possibly to some remaining contaminants species (H_2, O_2, H_2O…) on the platinum, due to a poor cleaning of its surface when the sample is pre-treated at room temperature (25 °C). As reported in the literature, platinum shows a preference for a linear mode of carbon monoxide adsorption [71]. Anyway, for low surface coverage, two IR bands are observed from spectroscopic data of CO adsorbed on Pt supported powders: at around 1870 and 2060 cm^{-1} [72–74]. These bands have been attributed either to CO adsorbed on various sites of the metal [71] or to linear (2060 cm^{-1}) and bridged (1870 cm^{-1}) forms of adsorbed CO [18, 75]. The microcalorimetric results, with rather similar adsorption heat values in a large domain, can suggest that the main adsorbed species, over all Pt/C catalysts, are linear, as may also be inferred from spectroscopic data [71, 73, 74]. However, the presence of surface oxygen functional groups (SOFGs) on the support could modify the strength of the Pt–CO bonds. Thus, the differences observed in between Pt/C catalysts for CO adsorption were attributed to the contribution of the support to the surface properties, knowing that electron-donating supports produce an enrichment of the electron density of metal atoms interacting with them [76], inducing changes in the chemisorption properties of the metal particles. Nørskov et al. [77] have also demonstrated that the heats of adsorption of a species is directly related to the local structure of the catalysts, the step sites are more active unless poisoned, and they bind the adsorbates more strongly. The heats of adsorption are closely related to the adsorbate-substrate bond strength. Furthermore, the differential heat of adsorption can be dependent on the surface coverage of the adsorbate due to the lateral adsorbate-adsorbate interactions or due to the surface heterogeneity [50].

In contrast to other techniques for studying adsorption, heat-flow calorimetry yields both kinetic and thermodynamic information. The kinetics of heat release during adsorption can be monitored by changes in the thermokinetic parameter, τ. The calorimetric signal decreases exponentially with the adsorption time after the maximum of each adsorption peak. This can be expressed in the form $D(t) = D_m \exp(-t/\tau)$, where $D(t)$ and D_m are the deviation of the calorimetric signal at time t and the maximum deviation, respectively. The thermokinetic parameter τ in this expression can thus be computed as the inverse of the slope of the logarithm of the evolved heat curve during the return to equilibrium, and depends mainly on the accessibility of the adsorption sites in the samples. Thus, it was found [65] that the pore architecture of Pt/C catalysts (e.g. pore volume and pore size distribution) influenced the kinetics of heat release during CO adsorption.

The accessibility of CO molecules to the adsorption sites increased with the mesoporosity of the catalyst. When the Pt/C catalyst is predominantly mesoporous, the

diffusion is not limited by movement of CO through micropores. More mesoporosity facilitates the creation of larger paths for diffusion, leading to an increased accessibility of CO molecules to the adsorption sites in the samples.

Different behaviour was also observed for Pt/C powders when their CO adsorption properties were studied [66, 67] after the catalysts were reduced at various temperatures. When the pre-treatment temperature was increased from 25 to 100 and further to 200 °C, the adsorptive properties of high loading Pt/C catalysts were influenced as shown for example in Fig. 12.6 [66]. Increasing the pre-treatment temperature provoked a decrease in the amount of chemisorbed carbon monoxide as well as in the values of differential heats of CO adsorption for the sample provided by E-Tek. These results were related with the changes in Pt particle sizes and dispersion as well as to a better cleaning of the catalyst surface when a higher pre-treatment temperature was used. This demonstrates once more that adsorption microcalorimetry is a powerful tool allowing the detection of different changes in the catalyst surface.

It has to be pointed out that not all the tested Pt/C samples presented the same behaviour for CO adsorption with increasing temperature of pre-treatment. Observation of the calorimetric profiles (Fig. 12.7) reveals a plateau at around 135 kJ/mol for Pt/C Tanaka, which did not change with increasing of reduction temperature.

The constant value of the plateau extends over a wide range of surface coverage, thus indicating a high homogeneity of the surface metal atoms of this sample for the CO adsorption. The drop in the differential heats at higher coverage is indicative of saturation of the accessible platinum metallic surface sites. The changing of the reduction conditions influenced only the total capacity (the length of plateau) of CO adsorption, which decreased with increasing pre-treatment temperature, due to the changes in Pt particle sizes and dispersion. Moreover, no differences in the adsorptive

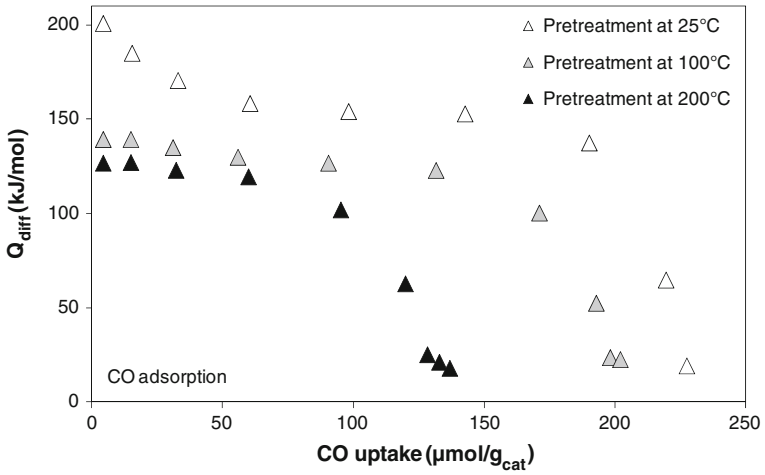

Fig. 12.6 Differential heats of CO adsorption at 30 °C as a function of surface coverage for Pt/C catalyst (E-Tek, lot#E 1280702) pre-treated at 25, 100 and 200 °C in static hydrogen (27 kPa) [66]

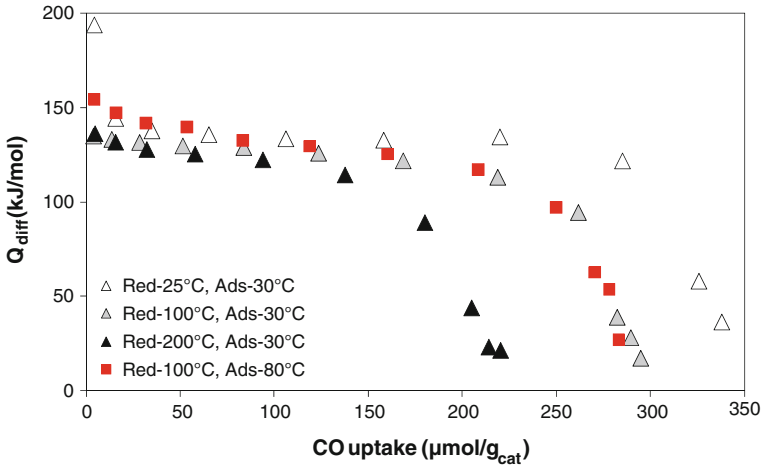

Fig. 12.7 Differential heats of CO adsorption at 30 and 80 °C as a function of surface coverage for Pt/C catalyst (Tanaka, lot 103-1341R) pre-treated at 25, 100 and 200 °C in static hydrogen (27 kPa)

properties of Pt/C catalyst for CO were observed when the adsorption temperature was increased from 30 to 80 °C and the same pre-treatment procedure was employed, which was the case for all studied powders.

When the thermokinetic parameter was measured, a more detailed characterization of the available sites for CO adsorption on the Pt/C surface was provided. For example, it was possible to differentiate reversible and irreversible adsorption processes. Because chemisorption may be a slow, irreversible process, involving activation of the adsorbate, a longer time and, therefore, a broader thermogram would distinguish such a process from a faster, reversible physisorption process. This feature was thus exploited to monitor the change in adsorption with coverage. As presented in Fig. 12.8, the adsorption process was initially slow and became slower, reaching a minimum of rate, before a significant acceleration of the process which was observed on approaching the physisorbed state at high coverage. The minimum rate appears as a maximum in a plot of the thermokinetic parameter as a function of the surface coverage, being indication of a change from irreversible to reversible adsorption.

As it can be seen in Fig. 12.8, the kinetic of CO adsorption on Pt based catalysts did not change when the adsorption and the pre-treatment were performed at higher temperature. As expected, the thermokinetic parameter firstly increases to reach a maximum and then slowly decreases showing that CO is almost completely irreversibly adsorbed on the surface of Pt-based catalyst. The amount held by the strong chemisorption sites at a certain adsorption temperature gives valuable information about the catalysts behaviour towards poisoning. Indeed, as deduced from volumetric data, 93 and 85 % of the total amount of CO was irreversibly adsorbed on Pt/C Tanaka catalyst for the powder pre-treated at 25 °C and CO adsorbed at 30 °C, and for the same sample pre-treated at 100 °C and CO adsorbed at 80 °C, respectively. Similar

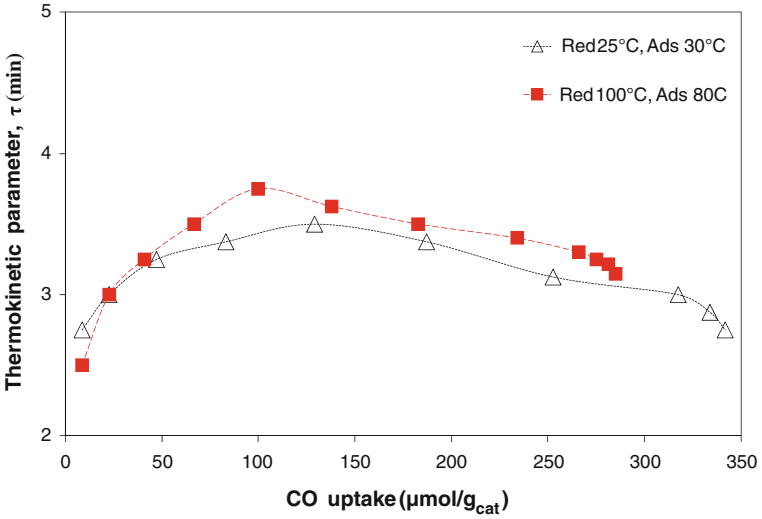

Fig. 12.8 Variation of the thermokinetic parameter, τ, versus CO uptake for Pt/C sample (Tanaka, lot 103-1341R)

results were also obtained for the catalysts provided by E-Tek and Johnson Matthey companies, with more than 90 % of CO irreversibly adsorbed for both powders.

A different and unexpected behavior was observed for the Pt/C catalyst provided by Johnson Matthey showing that the results obtained by direct adsorption calorimetric measurements provide accurate values of the heats of CO adsorption, and that they are directly related with the catalyst history (carbon used as support, the method of preparation). The calorimetric results obtained for this sample are given in Fig. 12.9 and Table 12.3.

The differential heat profiles of CO adsorption presented in Fig. 12.9 are very similar at low CO coverage (up to around 100 $\mu mol_{CO}/g_{cat}$) in spite of different reduction temperatures used. After a CO coverage of 100 $\mu mol_{CO}/g_{cat}$, when the catalyst was pretreated at 25 and 100 °C, an increase in the adsorption heats could be observed with increasing CO uptake, before a drastic drop to the values corresponding to weakly adsorbed CO (40 kJ/mol). The total metal stoichiometries at saturation are not influenced by increasing the pre-treatment temperature.

As can be seen in Table 12.3, the irreversibly chemisorbed amount of CO (n_{irrev}) can also be measured from the calorimetric studies. Obviously, this volume corresponds to the total amount held by the strong sites at the adsorption temperature over the catalysts. In order to accurately determine the chemisorbed amount from the overall adsorption isotherm, the catalyst was outgassed after the first adsorption run at the same temperature to remove the physically adsorbed amount, after which a new adsorption procedure was carried out to obtain a second isotherm. The difference between the first and second isotherm gives the extent of irreversible adsorption (n_{irrev}) at a given temperature. However, in the first approximation, the magnitude of

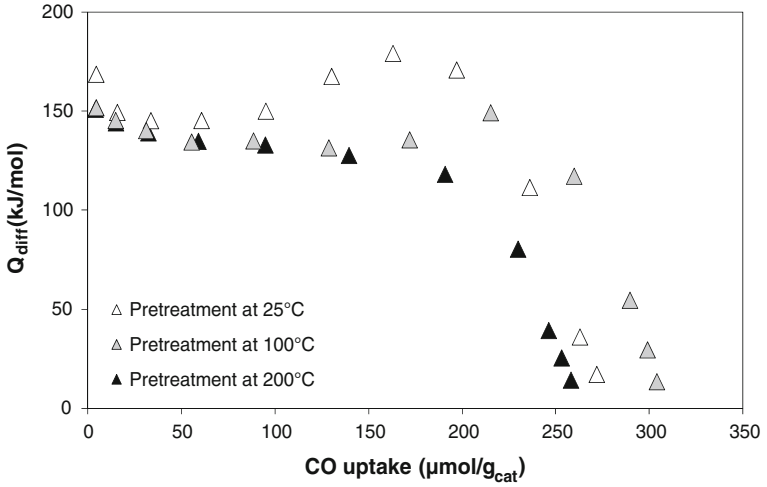

Fig. 12.9 Differential heats of CO adsorption at 30 °C as a function of surface coverage for Pt/C catalyst (Johnson Matthey, lot 128372001) pre-treated at 25, 100 and 200 °C in static hydrogen (27 kPa) [67]

Table 12.3 Data obtained from microcalorimetric measurements for Pt/C Johnson Matthey sample (lot 128372001)

Temperature of reduction (°C)	H_2 adsorption at 30 °C				CO adsorption at 30 °C			
	D (%)	Q_{init} [a] (kJ/mol)	H_2 uptake (µmol/g_{Pt})		D (%)	Q_{init} [a] (kJ/mol)	CO uptake (µmol/g_{Pt})	
			n_{total} [b]	n_{irrev} [c]			n_{total} [b]	n_{irrev} [c]
25	26.12	89	551	72	31.95	169	1413	1253
100	30.98	89	669	207	35.75	152	1744	1587
200	31.56	94	653	291	30.31	151	1490	1322

[a] Initial differential heats of H_2 and CO adsorption; [b] Amount of H_2 and CO adsorbed under an equilibrium pressure of 27 Pa; [c] Amount of irreversibly chemisorbed H_2 and CO under an equilibrium pressure of 27 Pa

the heat of adsorption can be considered as a simple criterion to distinguish between physical and chemical adsorption. As can be deduced from Table 12.3 which summarizes n_{irrev}, n_{total} as well as the dispersion obtained from the total amounts of H_2 and CO uptake at the monolayer, CO is almost completely irreversibly adsorbed on the surface of the Pt/C catalyst (i.e. 87, 91 and 89 % for the sample pre-treated at 25, 100 and 200 °C, respectively).

It was found that the available hydrogen adsorption sites have a broader site energy distribution, while the intermediate and low adsorption sites are almost not observed for carbon monoxide. The broader site energy distribution monitored by H_2 adsorption microcalorimetry can be attributed to the higher surface mobility of hydrogen.

From the data presented in Table 12.3, it is clear that at 30 °C an irreversible form of adsorbed hydrogen is detected on platinum, together with a reversible one for higher coverage. It means that carbon monoxide was adsorbed on the catalyst previously contacted with hydrogen. Even if the sample is evacuated before CO adsorption, CO was adsorbed on a surface partly covered with strongly bonded hydrogen which was not completely removed during outgassing under vacuum. It is evident from the presented data that the strong adsorption of CO at the Pt surface can directly block the surface active sites used for H_2 adsorption. As reported also in the literature [17], the representative mechanism of hydrogen adsorption containing small amounts of carbon monoxide can be expressed as follows:

$$H_2 + 2Pt \rightarrow 2Pt{-}H_{ads} \tag{12.4}$$

$$CO + Pt \rightarrow Pt{-}CO_{ads} \tag{12.5}$$

$$2CO + 2Pt{-}H_{ads} \rightarrow 2Pt{-}CO_{ads} + H_2 \tag{12.6}$$

The adsorption of CO occurs not only at bare Pt sites through reaction (12.5) but also at Pt hydride sites via reaction (12.6). This is not surprising, since the heats of adsorption of CO on Pt are much higher than that of irreversibly adsorbed hydrogen.

As observed in Fig. 12.9, up to coverage of about 100 $\mu mol_{CO}/g_{cat}$, the CO molecules are adsorbed on unoccupied active sites on the catalyst surface. At higher CO coverage, the noticed increase of differential heats can be attributed to the replacement of hydrogen irreversibly adsorbed by CO (reaction 12.6) which explains the different platinum dispersion found from H_2 and CO adsorption.

When the catalyst was pre-treated at a temperature of 200 °C, no increase of the heats was observed and similar values for the hydrogen and CO dispersion were found. This means that with increasing activation temperature, CO adsorption occurs on a reduced and clean surface. Therefore, for this catalyst, the temperature of pre-treatment does not seem to influence the adsorption capacity, but plays a role in the type of available sites on the surface. It has to be noted that the bell shaped profile was not observed for the other investigated catalyst which means that the adsorption properties are strongly dependent on the catalyst surface structure. Thus, the history of the investigated materials is of importance: platinum is supported on different carbons, in different quantities and possibly different preparation procedures have been used; which influenced its dispersion and orientation. All these features can be responsible as a whole for the different adsorptive properties of the studied materials. But, in spite of different differential heats profiles observed, there is no doubt that CO adsorbs quickly and essentially irreversibly on Pt even in the presence of pre-adsorbed hydrogen on the surface of catalyst. In the absence of CO, hydrogen adsorbs onto active platinum sites. Nevertheless, when only traces of CO are presented in the anode gas mixture, it will gradually accumulate on the platinum surface through a replacement reaction or a free site adsorption. Thus, the CO-poisoning arises from the adsorption of CO molecules on the platinum catalyst sites, which avoids the hydrogen to reach the platinum particles.

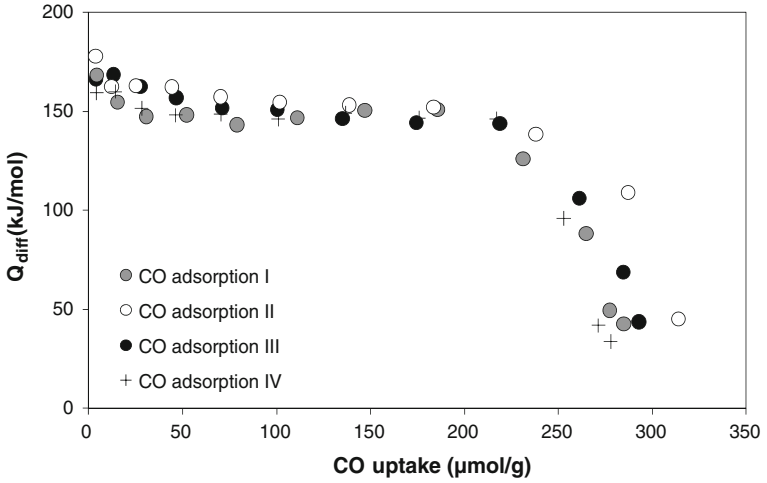

Fig. 12.10 Differential heats of CO adsorption at 80 °C as a function of surface coverage for Pt/C powder (Johnson Matthey, lot 128372001) pre-treated at 100 °C in static hydrogen (27 kPa) [67]

Finally, the response to several cycles poisoning-recovering has also been assessed by using the adsorption microcalorimetry. The poisoning degree of Pt/C and the catalysts regeneration was followed during four successive CO adsorption/desorption/readsorption cycles on the same bath of sample [65, 67]. For this, in between two successive CO adsorption runs, the catalysts were kept under air overnight and again reduced under static hydrogen before a new adsorption cycle. The results obtained for Pt/C Johnson Matthey, are given as example in Fig. 12.10. Here, the CO adsorption was performed at 80 °C after the catalyst was reduced at 100 °C. As it can be seen, this sample seems to be tolerant to CO poisoning in spite of the fact that CO binds strongly on Pt and cannot be desorbed at the operation temperature of PEM fuel cells (lower than 100 °C). The same result was obtained when a similar study was performed at room temperature [65]. This behaviour suggests that the platinum morphology, structure and adsorbed CO species are restored or remain unchanged, independently of the repeated exposure to air/H_2/CO. It was not the case for the other studied samples as shown in the same reference [65]. Differences appeared in the total amount of CO adsorbed after each cycle, which decreases considerably at the end of the experiments. The degree of catalyst poisoning by CO upon successive air/H_2/CO cycles varied between 2 and 30 % for different studied samples. The decrease in CO adsorption capacity, which means a decrease in the number of adsorption sites, can be attributed to an irreversible poisoning of the surface. No relation in between the loading of Pt and the tolerance to CO poisoning could be found. These results confirm that the surface chemistry of the catalyst affects the surface site energy distribution and consequently the adsorptive properties towards H_2 and CO. Thus it can be concluded that if the catalyst characteristics are well controlled, the reformate gas can be used as fuel for operation in PEMFC but an exhaustive control of CO must be anyway taken into account.

12.5 Summary

The CO poisoning effect on PEM fuel cells efficiency is still under active study. The detailed mechanism is still not well understood and there are contradictory observations that need to be clarified. The goal of our work was to verify if the adsorption microcalorimetry is an available technique for further understanding of the effects of impurities on hydrogen activation and hydrogen surface coverage of Pt/C catalysts used as anode in PEM fuel cells. It is evident that a correlation between poisoning effects and the adsorptive properties exists, the rate of the former being catalyst structure sensitive. The CO-poisoning can be a reversible process through air bleed at the anode and the injection of clean hydrogen. Anyway it was shown that the degree of recovery performances is directly related to the specific structure of the surface metallic atoms of the catalyst. It was proven that microcalorimetry technique is quite well developed and very useful in providing information on the strength and distribution of active sites for CO adsorption on the catalyst surface.

References

1. L. Carrette, K.A. Friedrich, U. Stimming, Fuel cells-fundamentals and applications. Fuel Cells **1**, 5–39 (2001)
2. S. Litster, G. McLean, PEM fuel cell electrodes. J. Power Sources **130**, 61–76 (2004)
3. A. Boudghene Stambouli, E. Traversa, Solid oxide fuel cells (SOFCs): a review of an environmentally clean and efficient source of energy. Renew. Sustain. Energy Rev. **6**, 433–455 (2002)
4. B.C.H. Steele, Material science and engineering: the enabling technology for the commercialisation of fuel cell systems. J. Mater. Sci. **36**, 1053–1068 (2001)
5. B.C.H. Steele, A. Heinzel, Materials for fuel-cell technologies. Nature **414**, 345–352 (2001)
6. R.A. Lemons, Fuel cells for transportation. J. Power Sources **29**, 251–264 (1990)
7. T. Yalcinoz, M.S. Alam, Improved dynamic performance of hybrid PEM fuel cells and ultracapacitors for portable applications. Int. J. Hydrogen Energy **33**, 1932–1940 (2008)
8. O. Erdinc, M. Uzunoglu, Recent trends in PEM fuel cell-powered hybrid systems: investigation of application areas, design architectures and energy management approaches. Renew. Sustain. Energy Rev. **14**, 2874–2884 (2010)
9. A. Bıyıkoğlu, Review of proton exchange membrane fuel cell models. Int. J. Hydrogen Energy **30**, 1181–1212 (2005)
10. M.L. Perry, R.M. Darling, S. Kandoi, T.W. Patterson, C. Reiser, in *Polymer Electrolyte Fuel Cell Durability*, ed. by F.N. Buchi, M. Inaba, T.J. Schmids (LLC, Springer Science and Business Media, New York , 2009), p. 405
11. H. Liu, F.D. Coms, J. Zhang, H.A. Gasteiger, A.B. LaConti, in *Polymer Electrolyte Fuel Cell Durability*, ed. by F.N. Buchi, M. Inaba, T.J. Schmids (LLC, Springer Science and Business Media, New York , 2009), p. 80
12. A. Midilli, M. Ay, I. Dincer, M.A. Rosen, On hydrogen and hydrogen energy strategies I: current status and needs. Renew. Sustain. Energy Rev. **9**, 255–271 (2005)
13. R. Jiang, H.R. Kunz, J.M. Fenton, Influence of temperature and relative humidity on performance and CO tolerance of PEM fuel cells with Nafion®-Teflon®-Zr$(HPO_4)_2$ higher temperature composite membranes. Electrochim. Acta **51**, 5596–5605 (2006)
14. S. Gottesfeld, J. Pafford, A new approach to the problem of carbon monoxide poisoning in fuel cells operating at low temperatures. J. Electrochem. Soc. **135**, 2651–2652 (1988)

15. J. Wu, X.Z. Yuan, J.J. Martin, H. Wang, J. Zhang, J. Shen, S. Wu, W. Merida, A review of PEM fuel cell durability: degradation mechanisms and mitigation strategies. J. Power Sources **184**, 104–119 (2008)
16. H.-F. Oetjen, V.M. Schmidt, U. Stimming, F. Trila, Performance data of a proton exchange membrane fuel cell using H_2/CO as fuel gas. J. Electrochem. Soc. **143**, 3838–3842 (1996)
17. X. Cheng, Z. Shi, N. Glass, L. Zhang, J. Zhang, D. Song, Z.-S. Liu, H. Wang, J. Shen, A review of PEM hydrogen fuel cell contamination: impacts, mechanisms, and mitigation. J. Power Sources **165**, 739–756 (2007)
18. J.Z. Zhang, Z. Liu, The effect of low concentrations of CO on H_2 adsorption and activation on Pt/C. Part 1: in the absence of humidity. J. Power Sources **195**, 3060–3068 (2010)
19. F.A. De Bruijn, D.C. Papageorgopoulos, E.F. Sitters, G.J.M. Janssen, The influence of carbon dioxide on PEM fuel cell anodes. J. Power Sources **110**, 117–124 (2002)
20. A. Pitois, A. Pilenga, G. Tsotridis, CO desorption kinetics at concentrations and temperatures relevant to PEM fuel cells operating with reformate gas and PtRu/C anodes. Appl. Catal. A **374**, 95–102 (2010)
21. B. Du, R. Pollard, J.F. Elter, M. Ramani, in *Polymer Electrolyte Fuel Cell Durability*, ed. by F.N. Buchi, M. Inaba, T.J. Schmids (LLC, Springer Science and Business Media, New York , 2009), pp. 341–366
22. L. Li, G. Wu, B.Q. Xu, Electro-catalytic oxidation of CO on Pt catalyst supported on carbon nanotubes pretreated with oxidative acids. Carbon **44**, 2973–2983 (2006)
23. H. Igarashi, T. Fujino, M. Watanabe, Hydrogen electro-oxidation on platinum catalysts in the presence of trace carbon monoxide. J. Electroanal. Chem. **391**, 119–123 (1995)
24. J.J. Baschuk, X.G. Li, Carbon monoxide poisoning of proton exchange membrane fuel cells. Int. J. Energy Res. **25**, 695–713 (2001)
25. K. Wang, H.A. Gasteiger, N.M. Markovic, On the reaction pathway for methanol and carbon monoxide electrooxidation on Pt-Sn alloy versus Pt-Ru alloy surfaces. Electrochim. Acta **41**, 2587–2593 (1996)
26. G. Garcıá, J.A. Silva-Chong, O. Guillén-Villafuerte, J.L. Rodríguez, E.R. González, E. Pastor, CO tolerant catalysts for PEM fuel cells. Spectroelectrochemical studies. Catal. Today **116**, 415–421 (2006)
27. J. Sobkowski, A. Czerwinski, Voltammetric study of CO and CO_2 adsorption on smooth and platinized platinum electrodes. J. Phys. Chem. **89**, 365–369 (1985)
28. B. Beden, C. Lamy, N.R. de Tacconi, J. Arvia, The electrooxidation of CO: a test reaction in electrocatalysis. Electrochim. Acta **35**, 691–704 (1990)
29. M. Hachkar, T. Napporn, J.-M. LeÂger, B. Beden, C. Lamy, An electrochemical quartz crystal microbalance investigation of the adsorption and oxidation of CO on a platinum electrode. Electrochim. Acta **41**, 2721–2730 (1996)
30. S.J. Lee, S. Mukerjee, E.A. Ticianelli, J. McBreen, Electrocatalysis of CO tolerance in hydrogen oxidation reaction in PEM fuel cells. Electrochim. Acta **44**, 3283–3293 (1999)
31. H. Steininger, S. Lehwald, H. Ibach, On the adsorption of CO on Pt(111). Surf. Sci. **123**, 264–282 (1982)
32. H. Hanawa, K. Kunimatsu, H. Uchida, M. Watanabe, In situ ATR-FTIR study of bulk CO oxidation on a polycrystalline Pt electrode. Electrochim. Acta **54**, 6276–6285 (2009)
33. T. Sato, K. Kunimatsu, H. Uchida, M. Watanabe, Adsorption/oxidation of CO on highly dispersed Pt catalyst studied by combined electrochemical and ATR-FTIRAS methods. Part 1: ATR-FTIRAS spectra of CO adsorbed on highly dispersed Pt catalyst on carbon black and carbon un-supported Pt black. Electrochim. Acta **53**, 1265–1278 (2007)
34. A. Pitois, J.C. Davies, A. Pilenga, A. Pfrang, G. Tsotridis, Kinetic study of CO desorption from PtRu/C PEM fuel cell anodes: temperature dependence and associated microstructural transformations. J. Catal. **265**, 199–208 (2009)
35. A.-K. Meland, S. Kjelstrup, Three steps in the anode reaction of the polymer electrolyte membrane fuel cell. Effect of CO. J. Electroanal. Chem. **610**, 171–178 (2007)
36. A. Auroux, in *Catalyst Characterization: Physical Techniques for Solid Materials*, ed. by B. Imelik, J.C. Vedrine (Plenum Press, New York, 1994), p. 611

37. P.C. Gravelle, Application of adsorption calorimetry to the study of heterogeneous catalysis reactions. Thermochim. Acta **96**, 365–376 (1985)
38. B.E. Spiewak, J.A. Dumesic, Microcalorimetric measurements of differential heats of adsorption on reactive catalyst surfaces. Thermochim. Acta **290**, 43–53 (1996)
39. V.E. Ostrovskii, Molar heats of chemisorption of gases at metals: review of experimental results and technical problems. Thermochim. Acta **489**, 5–21 (2009)
40. P.L. Llewellyn, G. Maurin, Gas adsorption microcalorimetry and modelling to characterise zeolites and related materials. C. R. Chim. **8**, 283–302 (2005)
41. G. Postole, A. Auroux, in Advances, in *Fluid Catalytic Cracking: Testing, Characterization, and Environmental Regulations*, ed. by M.L. Occelli (CRC Press Taylor & Francis Group, Boca Raton, 2010), pp. 199–256
42. A. Guerrero-Ruiz, A. Maroto-Valiente, M. Cerro-Alarcon, B. Bachiller-Baeza, I. Rodriguez-Ramos, Surface properties of supported metallic clusters as determined by microcalorimetry of CO chemisorption. Top. Catal. **19**, 303–311 (2002)
43. J. Silvestre-Albero, J.C. Serrano-Ruiz, A. Sepulveda-Escribano, F. Rodriguez-Reinoso, Modification of the catalytic behaviour of platinum by zinc in crotonaldehyde hydrogenation and iso-butane dehydrogenation. Appl. Catal. A **292**, 244–251 (2005)
44. J.C. Serrano-Ruiz, A. Lopez-Cudero, J. Solla-Gullon, A. Sepulveda-Escribano, A. Aldaz, F. Rodriguez-Reinoso, Hydrogenation of α, β unsaturated aldehydes over polycrystalline, (111) and (100) preferentially oriented Pt nanoparticles supported on carbon. J. Catal. **253**, 159–166 (2008)
45. A. Guerrero-Ruiz, P. Badenes, I. Rodriguez-Ramos, Study of some factors affecting the Ru and Pt dispersions over high surface area graphite-supported catalysts. Appl. Catal. A **173**, 313–321 (1998)
46. J.C. Serrano-Ruiz, A. Sepulveda-Escribano, F. Rodriguez-Reinoso, Bimetallic PtSn/C catalysts promoted by ceria: application in the nonoxidative dehydrogenation of isobutene. J. Catal. **246**, 158–165 (2007)
47. J. Ruiz-Martinez, A. Sepulveda-Escribano, J.A. Anderson, F. Rodriguez-Reinoso, Influence of the preparation method on the catalytic behavior of $PtSn/TiO_2$ catalysts. Catal. Today **123**, 235–244 (2007)
48. M.A. Vannice, L.C. Hasselbring, B. Sen, Direct measurements of heats of adsorption on platinum catalysts. J. Catal. **97**, 66–74 (1986)
49. J.C. Serrano-Ruiz, G.W. Huber, M.A. Sanchez-Castillo, J.A. Dumesic, F. Rodriguez-Reinoso, A. Sepulveda-Escribano, Effect of Sn addition to Pt/CeO_2-Al_2O_3 and Pt/Al_2O_3 catalysts: an XPS, ^{119}Sn Mössbauer and microcalorimetry study. J. Catal. **241**, 378–388 (2006)
50. D. Uner, M. Uner, Adsorption calorimetry in supported catalyst characterization: adsorption structure sensitivity on Pt/γ-Al_2O_3. Thermochim. Acta **434**, 107–112 (2005)
51. A. Tanksale, J.N. Beltramini, J.A. Dumesic, G.Q. Lu, Effect of Pt and Pd promoter on Ni supported catalysts-a TPR/TPO/TPD and microcalorimetry study. J. Catal. **258**, 366–377 (2008)
52. A. Maroto-Valiente, I. Rodriguez-Ramos, A. Guerrero-Ruiz, Determination of the surface states of metallic clusters supported on alumina using microcalorimetry of CO adsorption. Thermochim. Acta **379**, 195–199 (2001)
53. H. Kivrak, A. Mastalir, Z. Kiraly, D. Uner, Determination of the dispersion of supported Pt particles by gas-phase and liquid-phase measurements. Catal. Commun. **10**, 1002–1005 (2009)
54. R. Alcala, J.W. Shabaker, G.W. Huber, M.A. Sanchez-Castillo, J.A. Dumesic, Experimental and DFT studies of the conversion of ethanol and acetic acid on PtSn-based catalysts. J. Phys. Chem. B **109**, 2074–2085 (2005)
55. R.D. Cortright, J.A. Dumesic, Microcalorimetric, spectroscopic, and kinetic studies of silica supported Pt and Pt/Sn catalysts for isobutene dehydrogenation. J. Catal. **148**, 771–778 (1994)
56. R.D. Cortright, J.A. Dumesic, Effect of potassium on silica-supported Pt and Pt/Sn catalysts for isobutene dehydrogenation. J. Catal. **157**, 576–583 (1995)
57. N.D. Gangal, N.M. Gupta, R.M. Iyer, Microcalorimetric study of the adsorption and reaction of CO, O_2, CO+O_2, and CO_2 on NaX zeolite, Pt/NaX, and platinum metal: effect of oxidizing and reducing pre-treatment. J. Catal. **140**, 443–452 (1993)

58. S.B. Sharma, J.T. Miller, J.A. Dimesic, Microcalorimetric study of silica- and zeolite-supported platinum catalysts. J. Catal. **148**, 198–204 (1994)
59. F. Rodríguez-Reinoso, I. Rodríguez-Ramos, A. Guerrero-Ruiz, J.D. López-González, Platinum catalysts supported on activated carbons. Part I: Preparation and characterization. J. Catal. **99**, 171–183 (1986)
60. A. Sepúlveda-Escribano, F. Coloma, F. Rodríguez-Reinoso, Platinum catalysts supported on carbon blacks with different surface chemical properties. Appl. Catal. A **173**, 247–257 (1998)
61. S. Ćerný, Adsorption calorimetry on filaments, vacuum-evaporated films and single crystals of metals. Thermochim. Acta **312**, 3–16 (1998)
62. A.D. Karmazyn, V. Fiorin, S.J. Jenkins, D.A. King, First-principles theory and microcalorimetry of CO adsorption on the 211 surfaces of Pt and Ni. Surf. Sci. **538**, 171–183 (2003)
63. Y.Y. Yeo, L. Vattunoe, D.A. King, Calorimetric heats for CO and oxygen adsorption and for the catalytic CO oxidation reaction on Pt111. J. Chem. Phys. **106**, 392–403 (1997)
64. Y.Y. Yeo, L. Vattunoe, D.A. King, Energetics and kinetics of CO and NO adsorption on Pt100: restructuring and lateral interactions. J. Chem. Phys. **104**, 3810–3821 (1996)
65. G. Postole, S. Bennici, A. Auroux, Calorimetric study of the reversibility of CO pollutant adsorption on high loaded Pt/carbon catalysts used in PEM fuel cells. Appl. Catal. B **92**, 307–317 (2009)
66. G. Postole, S. Bennici, A. Auroux, Poisoning by CO of Pt/C commercial catalysts used in PEMFCs. A microcalorimetric study, in Proceedings of International Symposium on Fundamentals and Developments of Fuel Cells (FDFC) 2011 Conference, ISBN: 978-2-7466-2970-7 (2011).
67. G. Postole, A. Auroux, The poisoning level of Pt/C catalysts used in PEM fuel cells by the hydrogen feed gas impurities: the bonding strength. Int. J. Hydrogen Energy **36**, 6817–6825 (2011)
68. S. Cerny, M. Smutek, F. Buzek, The calorimetric heats of adsorption of hydrogen on platinum films. J. Catal. **38**, 245–256 (1975)
69. J.B. Lantz, R.D. Gonzalez, Development of a new isothermal calorimeter; heats of hydrogen adsorption on supported platinum versus crystallite size. J. Catal. **41**, 293–302 (1976)
70. J.M. Herrmann, M. Gravelle-Rumeau-Maillot, P.C. Gravelle, A microcalorimetric study of metal-support interaction in the Pt/TiO_2 system. J. Catal. **104**, 136–146 (1987)
71. P. Hollins, The influence of surface defects on the infrared spectra of adsorbed species. Surf. Sci. Rep. **16**, 51–94 (1992)
72. M. Primet, J.M. Basset, M.V. Mathieu, M. Prettre, Infrared study of CO adsorbed on Pt/Al_2O_3. A method for determining metal-adsorbate interactions. J. Catal. **29**, 213–223 (1973)
73. S.D. Jackson, B.M. Glanville, J. Willis, G.D. McLellan, G. Webb, R.B. Moyes, S. Simpson, P.B. Wells, R. Whyman, Supported metal catalysts: preparation, characterization, and function. Part II: carbon monoxide and dioxygen adsorption on platinum catalysts. J. Catal. **139**, 207–220 (1993)
74. D. Liu, G.H. Que, Z.X. Wang, Z.F. Yan, In situ FT-IR study of CO and H_2 adsorption on a Pt/Al_2O_3 catalyst. Catal. Today **68**, 155–160 (2001)
75. M. Primet, J.M. Basset, M.V. Mathieu, M. Prettre, Infrared investigation of hydrogen adsorption on alumina-supported platinum. J. Catal. **28**, 368–375 (1973)
76. P. Gallezot, D. Richard, Selective hydrogenation of α, ß-unsaturated aldehydes. Catal. Rev. Sci. Eng. **40**, 81–126 (1998)
77. J.K. Nørskov, T. Bligaard, A. Logadottir, S. Bahn, L.B. Hansen, M. Bollinger, H. Bengaard, B. Hammer, Z. Slivancanin, M. Mavrikakis, Y. Xu, S. Dahl, C.J.H. Jakobsen, Universality in heterogeneous catalysis. J. Catal. **209**, 275–278 (2002)